

Expansion tomography for large volume tissue imaging with nanoscale resolution: supplement

**RUIXI CHEN,^{1,2} XIAOFENG CHENG,^{1,2} YONGSHENG ZHANG,^{1,2}
XIONG YANG,^{1,2} YU WANG,^{1,2} XIULI LIU,^{1,2,3} AND SHAOQUN
ZENG^{1,2,4}**

¹*Britton Chance Center for Biomedical Photonics, Wuhan National Laboratory for Optoelectronics
Huazhong University of Science and Technology, Wuhan 430074, China*

²*MoE Key Laboratory for Biomedical Photonics, Collaborative Innovation Center for Biomedical
Engineering, School of Engineering Sciences, Huazhong University of Science and Technology, Wuhan
430074, China*

³*xliu@hust.edu.cn*

⁴*sqzeng@mail.hust.edu.cn*

This supplement published with The Optical Society on 13 August 2021 by The Authors under the terms of the [Creative Commons Attribution 4.0 License](https://creativecommons.org/licenses/by/4.0/) in the format provided by the authors and unedited. Further distribution of this work must maintain attribution to the author(s) and the published article's title, journal citation, and DOI.

Supplement DOI: <https://doi.org/10.6084/m9.figshare.15123999>

Parent Article DOI: <https://doi.org/10.1364/BOE.431696>

**Expansion tomography for large volume tissues
imaging with nanoscale resolution: supplemental
document**

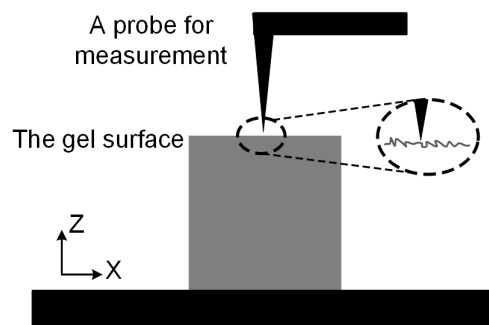


Fig. S1 Scheme of testing the sectioning surface flatness

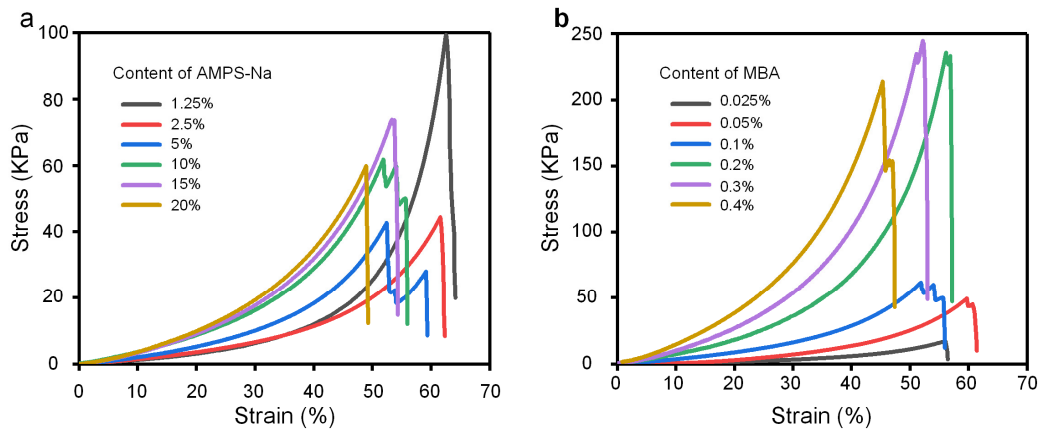


Fig. S2 The stress-strain curves of ExT hydrogels under compress test. (a) The stress-strain curves of ExT hydrogels with different concentration of AMPS-Na. (b) The stress-strain curves of ExT hydrogels with different concentration of MBA.

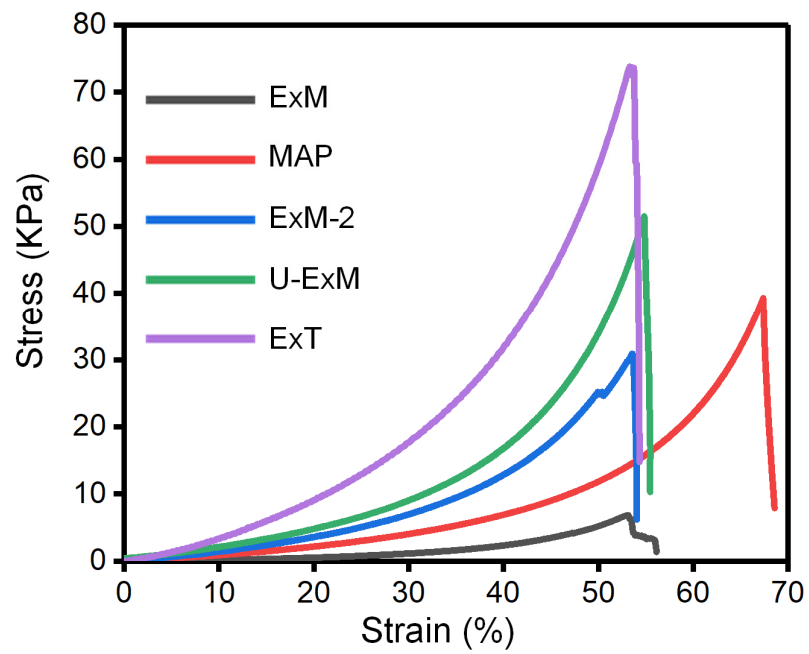


Fig. S3 Stress-strain curves for different expansion gel recipes presented in Fig. 2e.

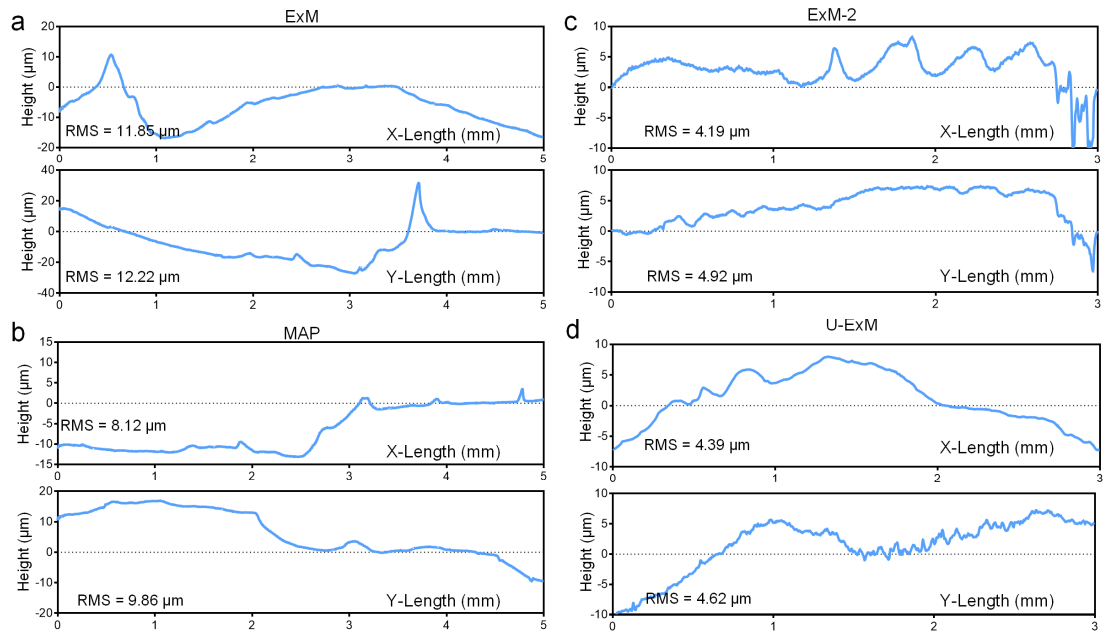


Fig.S4 Measurements of surface evenness of various hydrogel after continuous sectioning with a vibratome. X is the direction of sectioning and Y is perpendicular to the direction of sectioning.

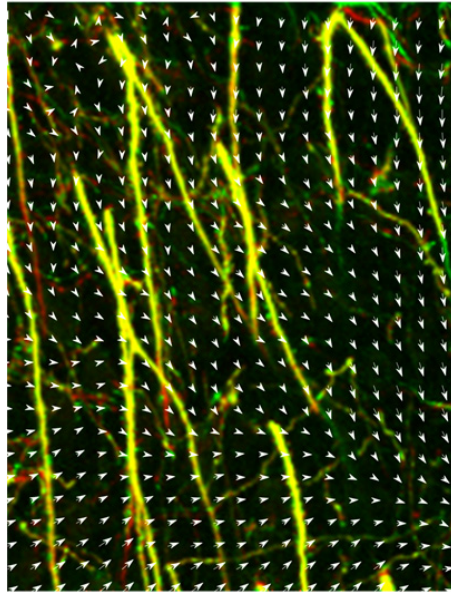


Fig. S5 Overlay of pre-expansion image (green) and post-expansion image (red) after alignment of the post-expansion image using similarity registration. Related to Fig. 2a.

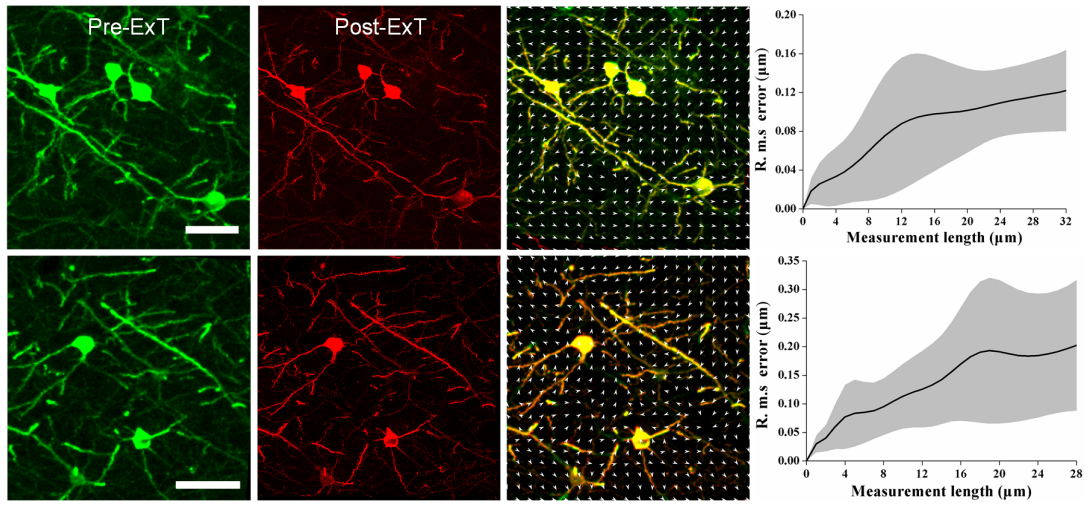


Fig S6. Overlay of pre-expansion image (green) and post-expansion image (red) after alignment of the post-expansion image using similarity registration. Arrows indicate deformation vectors to align the post-expansion image to the pre-expansion image. Scale bar: 50 μm

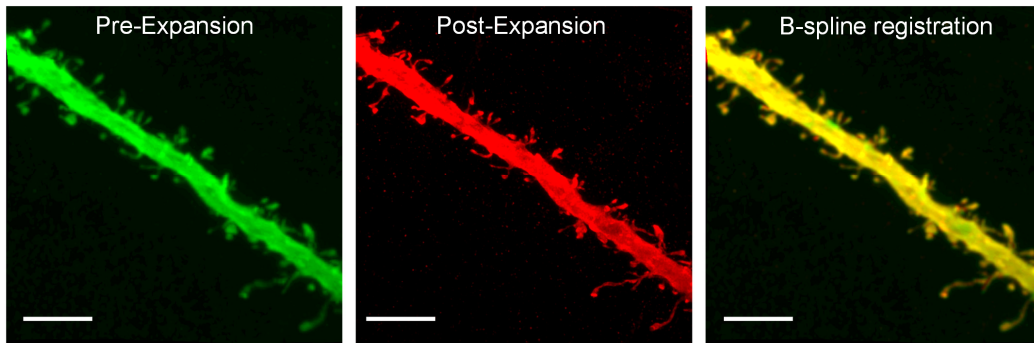


Fig S7. Overlay of pre-expansion image (green) and post-expansion image (red) after alignment of the post-expansion image using similarity registration. The image was obtained at a magnification of 63 \times oil immersion objective, NA=1.46. Scale bar: 5 μ m

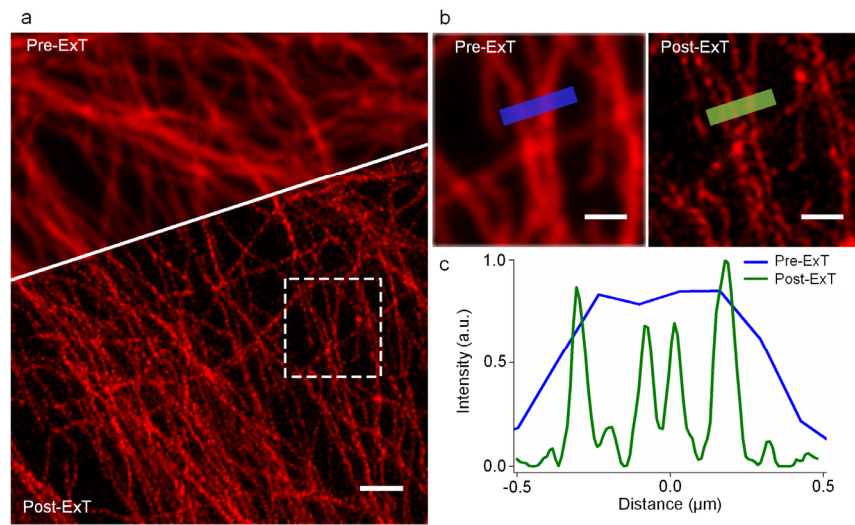


Fig. S8 U2OS cell immunostained for tubulin and partially overlaid with corresponding pre-expansion image (top). The specimen was treated with expansion protocol. $F=4.47$. (b) Zoomed-in view of boxed region in (a) showing corresponding pre-expansion and post-expansion. (c) images of tubulin signal along with corresponding (b) line profiles.

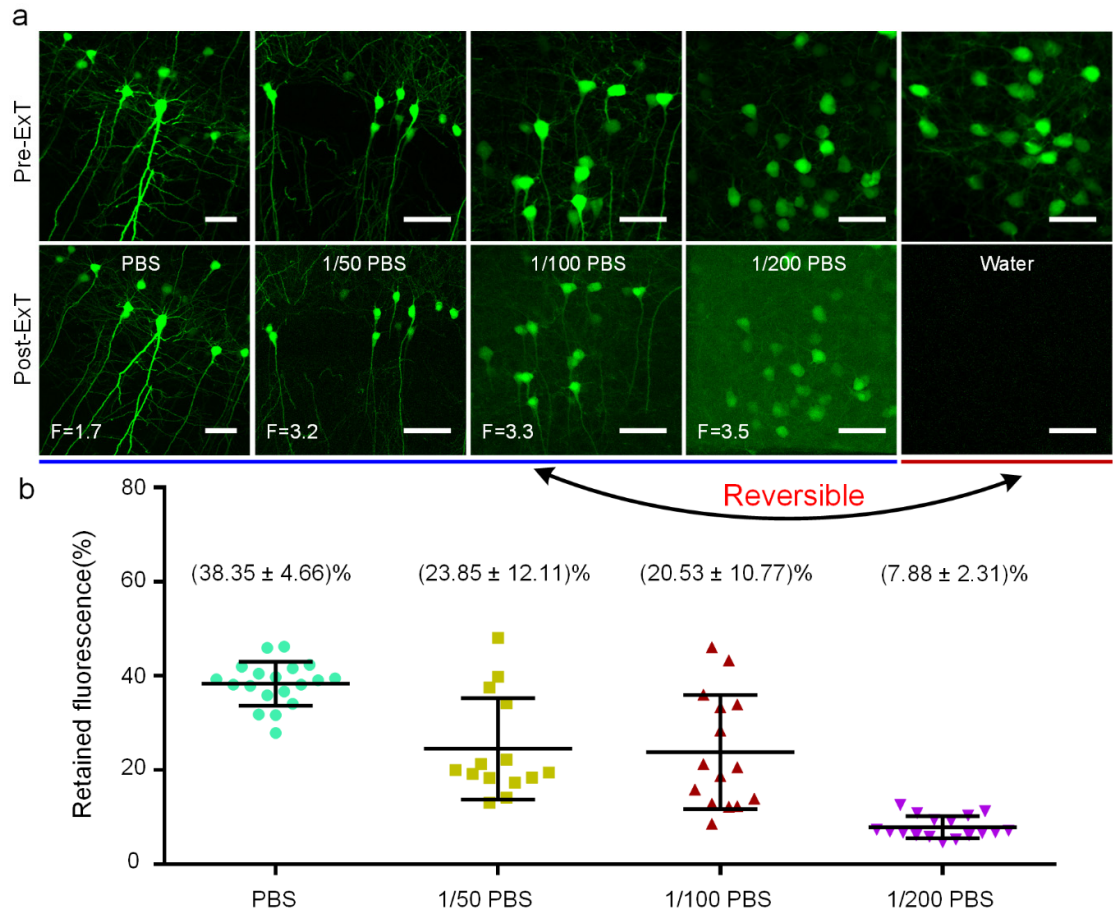


Fig. S9 Fluorescence changes of GFP samples after expansion with ExT hydrogel. (a) The top row shows images of GFP brain slices pre-expansion. The bottom row shows images of GFP brain slices after ExT hydrogel treatment and then expansion in different concentration of PBS solution and DI water. (1/50 PBS means a 50-fold dilution of the 1×PBS solution. Similarly, 1/100 PBS means a 100-fold dilution of the 1×PBS solution; 1/200 PBS means a 200-fold dilution of the 1×PBS solution). (b) Fluorescence persistence of GFP protein after expansion in various concentration of PBS (mean ± s.d., n = 30 somas from four brain slices). Scale bar: 50 μm.

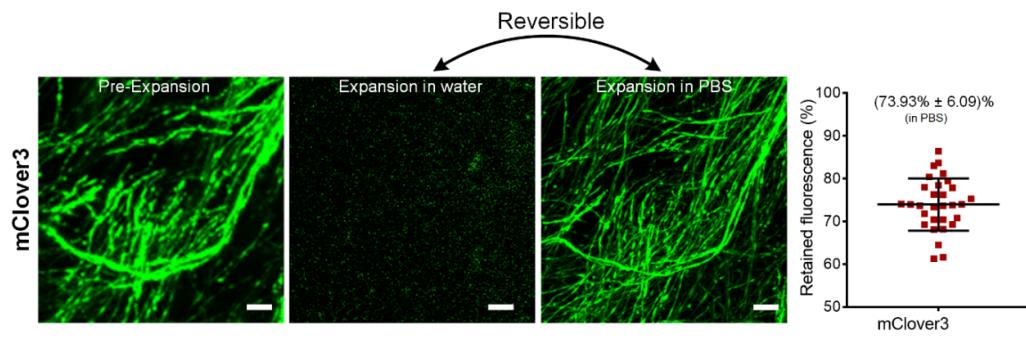


Fig. S10 Fluorescence changes of mClover3 samples after expansion in DI water and PBS. The fluorescence persistence of mClover3 protein expanded in PBS is $(73.93 \pm 6.09)\%$ (mean \pm s.d., $n = 30$ somas from four brain slices). Scale bar: 20 μm .

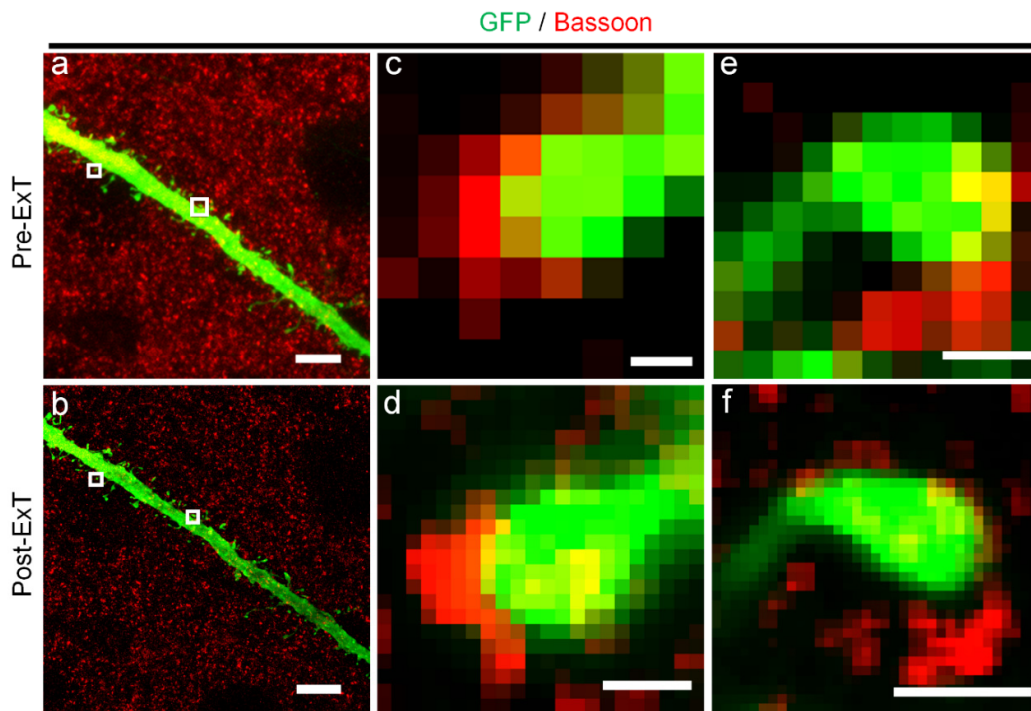


Fig. S11 Image of GFP (dendritic spines) and presynaptic marker bassoon. (a) pre-ExtT, (b) post-ExtT. (c, e) Enlargements of insets (white boxes) from (a). (d, f) Enlargements of insets (white boxes) from (b). Scale bar: (a)-(b) 5 μm, (c)-(d) 200 nm, (e)-(f) 500 nm.

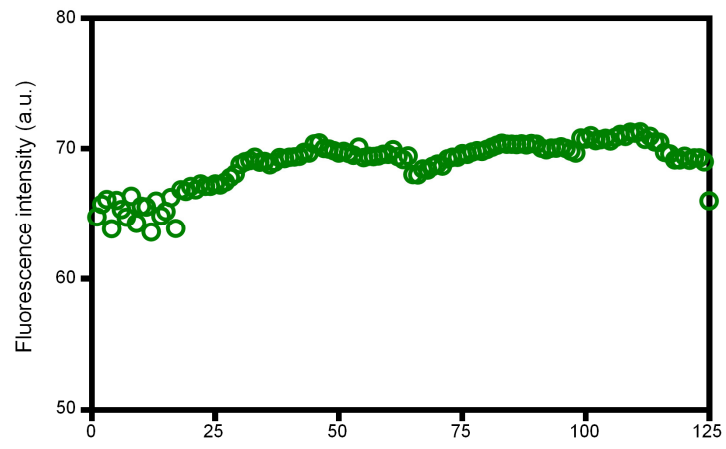


Fig. S12 Fluorescence intensity distribution in 50- μm slices.

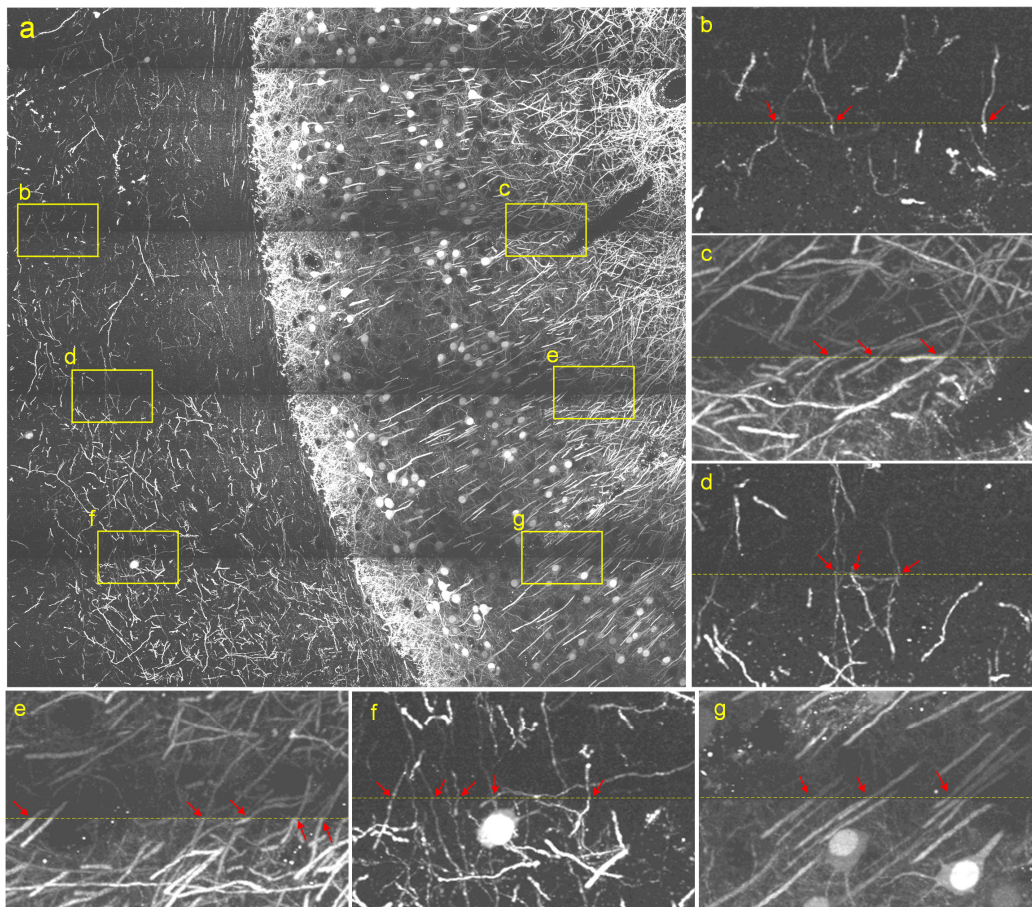


Fig. S13. The demonstration of continuous nerve fibers across the stitch. (a) A raw image of a layer that included multiple stitches.(b-g) Zoomed-in views of boxed regions in (a). Six stitches regions were selected as representatives to demonstrate the continuity of nerve fibers. The yellow dotted lines represent stitches, and red arrows represent locations of nerve fibers across the stitches.

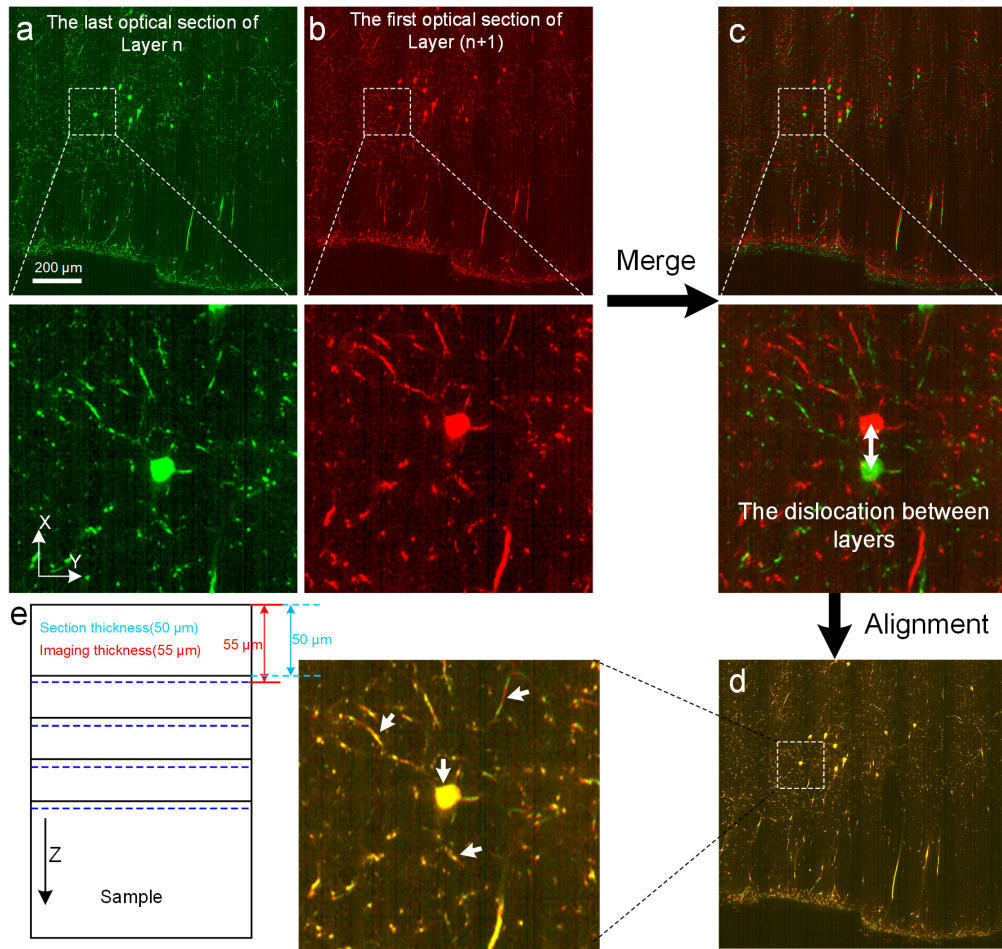


Figure S14 Layer-to-layer misalignment (a, b and c) and alignment correction (d) in sectioning imaging.

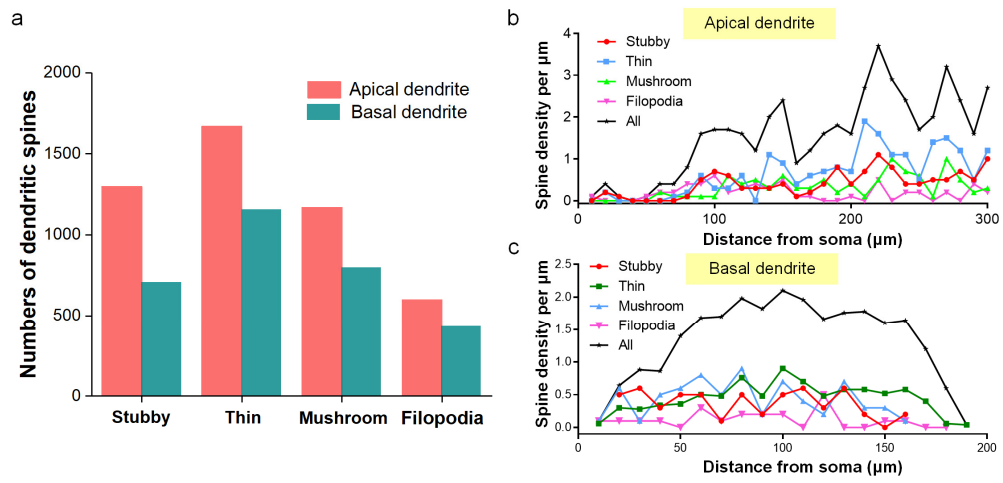


Fig. S15 Dendritic spines statistics. (a) Statistics on the number of dendritic spines in different classifications. (b) Density statistics of dendritic spines of apical dendrites. (c) Dendritic spines density statistics of basal dendrites.

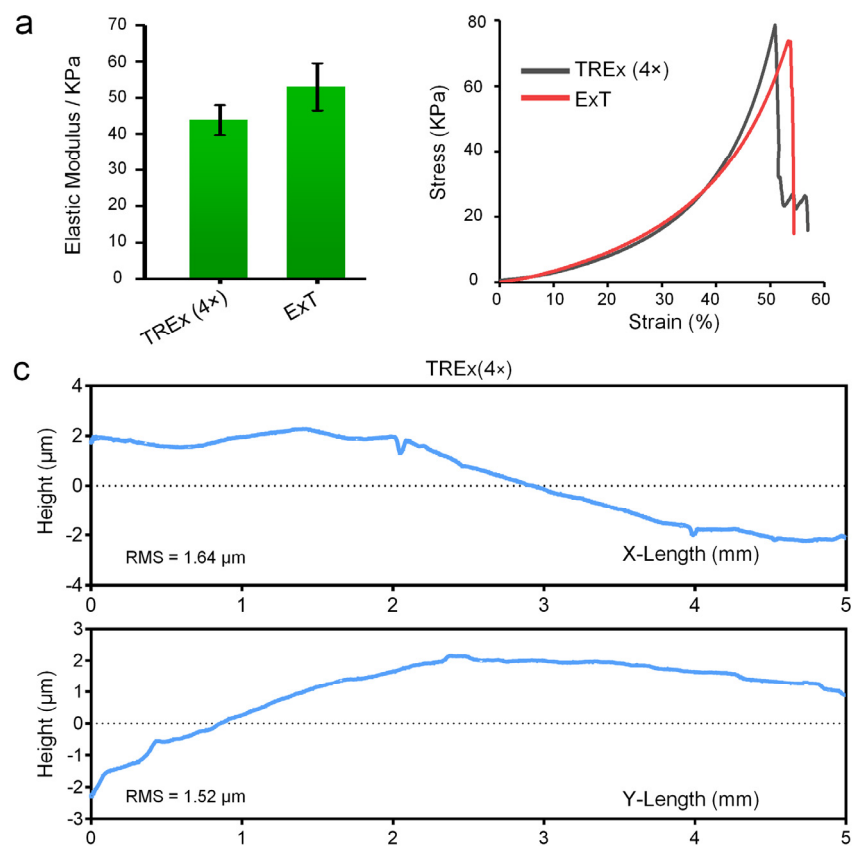


Fig. S16 Measurements of the elastic modulus (a), the stress-strain curve (b) and surface flatness after-slicing of TREx (4 \times) gel [1].

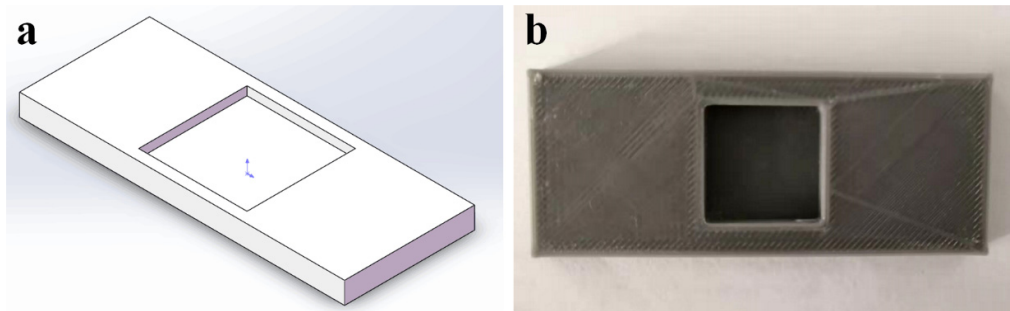


Fig. S17 A mold for gel polymerization of brain blocks. (a) Schematic diagram of 3D printing. (b) 3D printed physical pictures. The height of the groove in the mold can be adjusted according to the size of the sample.

Table S1. Monomer solution recipe of ExT gel.

AM (wt%)	AMPS-Na (wt%)	MBA (wt%)	Expansion Factor (F)	Elastic Modulus (E, kPa)	The integral area of the curve	
10	1.25	0.1	2.71 ± 0.05	16.5 ± 2.8	1084.41	
	2.5		3.23 ± 0.08	19.0 ± 3.7	696.12	
	5		3.42 ± 0.1	28.0 ± 3.5	768.78	
	10		4.19 ± 0.21	47.4 ± 4.2	1142.30	
	15		4.23 ± 0.22	53.0 ± 6.5	1165.87	
	20		4.20 ± 0.19	55.1 ± 5.1	909.96	
	10	10	0.025	6.8 ± 0.24	9.4 ± 3.6	253.56
			0.05	5.39 ± 0.23	19.3 ± 3.8	769.73
			0.1	4.19 ± 0.19	47.4 ± 4.2	1142.30
			0.2	3.31 ± 0.13	93.2 ± 5.6	3234.93
			0.3	2.76 ± 0.10	152.2 ± 7.1	3524.72
			0.4	0.83 ± 0.09	239.7 ± 9.3	3219.65

Table 2. Performance of selected secondary antibody dyes in ExT gel.

Dyes	Host species	E _x max, nm	E _m max, nm	Fluorescence preservation (%)	Source	Catalog #
Alexa 405	Goat anti rabbit	400	419	62.58 ± 5.82	Thermo Fisher	A-31556
Alexa 488	Goat anti rabbit	495	519	67.88 ± 6.02	Thermo Fisher	A-11008
CF 488	Goat anti rabbit	490	515	82.07 ± 6.60	Sigma-Aldrich	SAB4600044
Alexa 546	Donkey anti goat	556	573	96.92 ± 9.76	Thermo Fisher	A-11056
Alexa 568	Goat anti mouse	578	603	84.91 ± 11.88	Thermo Fisher	A-21124
CF 568	Goat anti rabbit	562	583	91.78 ± 10.32	Sigma-Aldrich	SAB4600084
Alexa 594	Goat anti rabbit	590	617	76.62 ± 6.87	Thermo Fisher	A-11012
Cy 3	Goat anti rabbit	550	570	68.46 ± 5.46	Jackson Laboratory	111-165-003
Cy 5	Goat anti rabbit	645	664	35.39 ± 3.37	Jackson Laboratory	111-175-144
Alexa 647	Donkey anti goat	650	665	29.27 ± 4.10	Thermo Fisher	A-21447

References

1. H. Damstra, B. Mohar, M. Eddison, A. Akhmanova, L. Kapitein, and P. Tillberg, "Visualizing cellular and tissue ultrastructure using Ten-fold Robust Expansion Microscopy (TREx)," bioRxiv. doi:10.1101/2021.02.03.428837 (2021).